

Dissociative ionization of H_2^+ by fast-electron impact: Use of a two-center continuum wave function

B. Joulakian,¹ J. Hanssen,¹ R. Rivarola,² and A. Motassim¹

¹*Institut de Physique, Laboratoire de Physique Moléculaire et des Collisions, Université de Metz, Technopôle 2000, 1 Rue Arago, 57078 Metz Cedex 3, France*

²*Instituto de Fisica Rosario (Consejo Nacional de Investigaciones Cientificas y Técnicas y Universidad Nacional de Rosario), Avenida Pellegrini 250, 2000 Rosario, Argentina*

(Received 26 December 1995)

The differential cross section of the dissociative ionization of H_2^+ by fast (2-keV) electron impact is determined theoretically using a two-center continuum wave function for the slow (50-eV) ejected electron satisfying the correct boundary conditions. The variation of the sevenfold differential cross section with the scattering angle for fixed molecular alignment shows diffraction patterns, which differ from those obtained by the multicenter atomic model of Messiah. The effect of the molecular alignment is studied for small, intermediate, and large scattering angles. This reveals preferential directions for the internuclear axis. [S1050-2947(96)08008-0]

PACS number(s): 34.80.Dp

I. INTRODUCTION

The dissociative ionization of H_2^+ by electron impact is one of the basic problems in the domain of $(e, 2e)$ reactions. It is actually the subject of a growing interest because of the rapid development of multiple coincidence detection techniques. The detection in coincidence with the scattered and ejected electrons and one of the protons can deliver information about the electronic structure and the mechanism of simultaneous ionization and dissociation, and permits us to study the dependence of the differential cross section on the orientation of the internuclear axis determined by the direction of one of the emerging protons. These types of coincidence detections are already performed in collision experiments involving multiply charged ionic projectiles and the hydrogen molecules [1–3].

Fundamental studies on the ionization of diatomic molecules by electrons are less frequent than those of atoms [4,5], especially in the theoretical domain, in spite of the fact that gases are found abundantly in diatomic molecular form. This could be explained by the fact that theoretically the basic problem of the scattering of an electron by two Coulomb centers has not yet been described by an appropriate approximation. The problem of the electron in the Coulomb field of two fixed nuclei is largely studied for the bound electronic states [6–9], where different types of wave functions [linear combination of atomic orbitals (LCAO), diatomic orbitals (DO), universal basis, etc.] are proposed. In spite of the separability of the Schrödinger equation in spheroidal coordinates, no closed exact analytical wave functions for the continuum states exist. In the multicenter scattering problem, Messiah [10] proposes, for large internuclear distances, the consideration of one-center wave functions in the calculation of the transition matrix elements. This method was recently applied to the electron-capture problem of multiply charged ions from H_2 by [1–3,11] and to the dissociative ionization of H_2^+ by some of us [12]. The main difficulty with this atomic model is that the orthonormalization

(in a box) of the final-state wave function is not clearly guaranteed, and the boundary conditions are satisfied only from the one-center point of view.

In this paper, we propose, for the slow (50-eV) ejected electron, a description that satisfies the correct asymptotic conditions based on a Pluvillage-type [13] analysis, by taking a product of two functions that take into account the two scattering centers. We adopt a plane-wave description of the incident and the scattered rapid (2-keV) electron. This is a reasonable approximation at high incident energy values. Moreover, our first aim here is to compare the differential cross sections of the dissociative ionization of H_2^+ , obtained under the same conditions with our procedure, to those obtained by the Messiah's model in [12], where plane waves were also used for the incident and the scattered electrons.

II. THEORY

We define in Fig. 1(a) the system of axes, whose origin coincides with the center of the H_2^+ diatomic system. The z axis is parallel to the direction of the impinging electron. The direction of the internuclear axis is determined by θ_ρ and φ_ρ , the polar and the azimuthal angles, respectively, which are supposed to be fixed during the ionization process, together with the internuclear distance ρ considered in its equilibrium value. We will consider that the collision time is much smaller than the period of the rotational and vibrational motions. Figure 1(b) shows the positions of the two nuclei, and that of the bound and incoming electrons.

The differential cross section, in a general out-of-plane detection of the two electrons and one of the H^+ , is sevenfold and is given by

$$\sigma^{(7)} = \frac{d^7\sigma}{d\Omega_\rho d\Omega_e d\Omega_s d(k_s^2/2)} = \frac{(2\pi)^4 k_e k_s}{k_i} |T_{fi}|^2, \quad (1)$$

where the Ω , Ω_e and the k_s , k_e represent, respectively, the solid angles and the moduli of the wave vectors of the scattered and the ejected electrons. This should be divided by

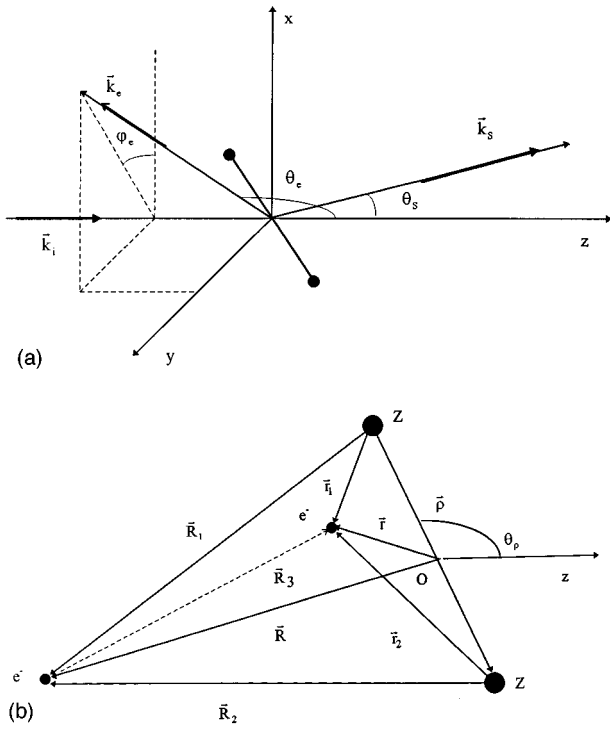


FIG. 1. (a) The reference frame with the different wave vectors \mathbf{k}_i , \mathbf{k}_s , and \mathbf{k}_e representing the incident, scattered, and the ejected electrons, respectively. θ_s , θ_e denote the scattering and the ejection angles, respectively. (b) The different position vectors of the incident and the bound electrons with respect to the two nuclei.

4π , if all the directions of the internuclear axis are considered to be equally probable. The conservation of the energy for fixed ρ gives

$$\frac{k_i^2}{2} + \frac{1}{\rho} = I^+ + \frac{k_s^2}{2} + \frac{k_e^2}{2} + 2E_p, \quad (2)$$

where I^+ represents the ionization energy and E_p the kinetic energy of an out-coming H^+ atom. The T matrix element T_{fi} is given in the case of an unpolarized electron beam by

$$T_{fi} = \frac{1}{4} |p+q|^2 + \frac{3}{4} |p-q|^2, \quad (3)$$

with

$$p = \langle \Psi_f^-(\mathbf{R}, \mathbf{r}) | V | \Psi_i(\mathbf{R}, \mathbf{r}) \rangle \quad (4)$$

and

$$q = \langle \Psi_f^-(\mathbf{r}, \mathbf{R}) | V | \Psi_i(\mathbf{R}, \mathbf{r}) \rangle, \quad (5)$$

with

$$p(\mathbf{k}_s, \mathbf{k}_e) = q(\mathbf{k}_e, \mathbf{k}_s). \quad (6)$$

Here the integration runs over all space coordinates designated by \mathbf{R} for the incident electron and \mathbf{r} for the bound one. V represents the interaction between the incident electron and the target H_2^+ [Fig. 1(b)]:

$$V = -\frac{Z}{R_1} - \frac{Z}{R_2} + \frac{1}{R_3}. \quad (7)$$

A. The initial state

For the collision by fast electrons we will describe the initial state by a product of a plane wave and a variational two-parameter solution of the $1\sigma_g$ fundamental state of H_2^+ ,

$$|\Psi_i\rangle = \frac{e^{i\mathbf{k}_i \cdot \mathbf{R}}}{(2\pi)^{3/2}} \Phi_{1\sigma_g}(\mathbf{r}, \rho), \quad (8)$$

with

$$\phi_{1\sigma_g}(\mathbf{r}, \rho) = N(\rho) \{ e^{-ar_1} e^{-br_2} + e^{-br_1} e^{-ar_2} \}, \quad (9)$$

where r_1 and r_2 represent the distances from the two nuclei [Fig. 1(b)], $a=0.224\,086$, and $b=1.136\,03$ are variational parameters that we have determined for the equilibrium internuclear distance $\rho=2$ a.u. and $N(\rho)=1.2434$. As we show below, the use of a wave function of this type for the ground state of H_2^+ is necessary to ensure convergence in the basic integrals [Eq. (19)].

B. The final state

In the final state, the scattered fast electron will be described by a plane-wave solution, and the ejected electron by the two-center continuum (TCC) wave function given by

$$\chi(\mathbf{r}_1, \mathbf{r}_2) = \frac{e^{i\mathbf{k}_e \cdot \mathbf{r}}}{(2\pi)^{3/2}} C(\mathbf{k}_e, \mathbf{r}_1) C(\mathbf{k}_e, \mathbf{r}_2), \quad (10)$$

with

$$C(\mathbf{k}_e, \mathbf{r}_j) = \exp(-\pi\alpha_e/2) \Gamma(1-i\alpha_e)_1 \times F_1(i\alpha_e, 1; -i(k_e r_j + \mathbf{k}_e \cdot \mathbf{r}_j)) \quad (11)$$

and $\alpha_e = -1/k_e$. This is inspired from the Pluvillage-type treatment [9] of the heliumlike systems, where one of the nuclei of H_2^+ replaces the second electron in the equation of He. Now in the asymptotic limit,

$$\lim_{r_1, r_2 \rightarrow \infty} [\chi(\mathbf{r}_1, \mathbf{r}_2)] = (2\pi)^{-3/2} \exp\{i\mathbf{k}_e \cdot \mathbf{r} + 2\alpha_e \ln(k_e r + \mathbf{k}_e \cdot \mathbf{r})\}, \quad (12)$$

which is the exact limit of the outgoing wave in the field of the two nuclei. The final state will be thus given by

$$\Psi_f^-(\mathbf{R}, \mathbf{r}) = \frac{e^{i\mathbf{k}_s \cdot \mathbf{R}}}{(2\pi)^{3/2}} \chi(\mathbf{r}_1, \mathbf{r}_2). \quad (13)$$

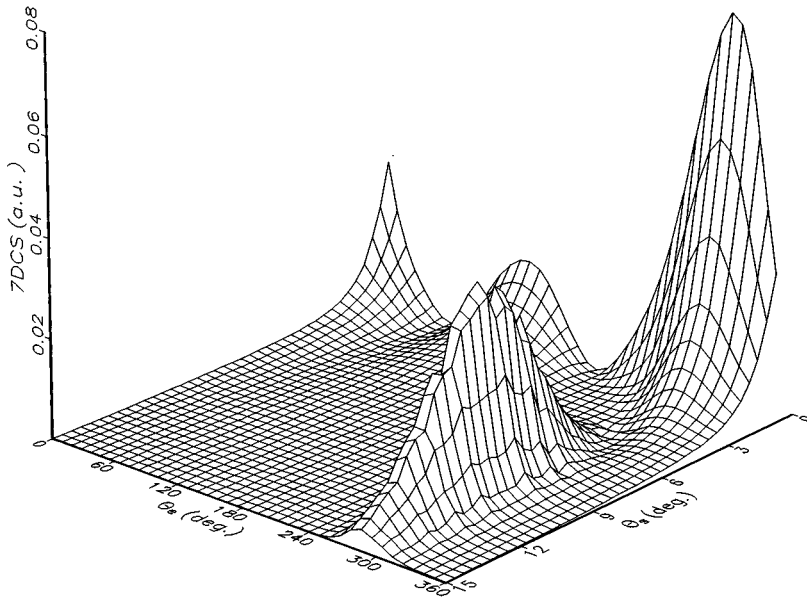


FIG. 2. The sevenfold differential cross section (7DCS) of the $(e, 2e)$ ionization of H_2^+ in terms of the ejection angle, θ_e , and the scattering angle, θ_s . The incident and the ejected electron energies are 2 keV and 50 eV, respectively. The internuclear axis is at 135° with respect to the incidence direction.

C. The transition amplitude

Replacing Eqs. (8) and (13) in Eq. (4), we obtain

$$p = \frac{N(\rho)}{2\pi^{9/2}} \exp(-\pi\alpha_e) [\Gamma(1+i\alpha_e)]^2 [I(a,b) + I(b,a)], \quad (14)$$

where

$$I(a,b) = -Z\{I_1(a,b) + I_2(a,b)\} + I_3(a,b) \quad (15)$$

with

$$\begin{aligned} I_j(a,b) = & \int \frac{d\mathbf{R}}{R_j} d\mathbf{r} e^{i\mathbf{K}\cdot\mathbf{R}} e^{-i\mathbf{k}_e\cdot\mathbf{r}} e^{-ar_1} \\ & \times {}_1F_1(-i\alpha_e, 1; i(k_e r_1 + \mathbf{k}_e \cdot \mathbf{r}_1)) e^{-br_2} \\ & \times {}_1F_1(-i\alpha_e, 1; i(k_e r_2 + \mathbf{k}_e \cdot \mathbf{r}_2)), \end{aligned} \quad (16)$$

where $\mathbf{K} = \mathbf{k}_i - \mathbf{k}_s$ represents the momentum transfer. Using the Fourier transform for one of the centers, as shown in the Appendix, and considering that $\mathbf{R} = \mathbf{R}_2 + \boldsymbol{\rho}/2 = \mathbf{R}_1 - \boldsymbol{\rho}/2$, $\mathbf{r} = \mathbf{r}_2 + \boldsymbol{\rho}/2 = \mathbf{r}_1 - \boldsymbol{\rho}/2$, and $\mathbf{R}_3 = \mathbf{R} - \mathbf{r}$, we could reduce this integral into a three-dimensional integral having the following form:

$$\begin{aligned} I_j(a,b) = & \frac{e^{[i(s_j\mathbf{K} - \mathbf{k}_e) \cdot (\boldsymbol{\rho}/2)]}}{2\pi^2 K^2} \int d\boldsymbol{\tau} e^{i\boldsymbol{\tau} \cdot \boldsymbol{\rho}} W(\mathbf{k}_e, \boldsymbol{\tau}, a) \\ & \times W(\mathbf{k}_e, -\boldsymbol{\eta}_j \mathbf{K} - \boldsymbol{\tau} + \mathbf{k}_e, b) \end{aligned} \quad (17)$$

with

$$\begin{aligned} s_j = -1, \quad \eta_j = 0 & \quad \text{for } j=1, \\ s_j = 1, \quad \eta_j = 0 & \quad \text{for } j=2, \\ s_j = 1, \quad \eta_j = 1 & \quad \text{for } j=3, \end{aligned} \quad (18)$$

$$W(\mathbf{k}, \mathbf{q}, \lambda) = \int d\mathbf{r} e^{-i\mathbf{q}\cdot\mathbf{r}} e^{-\lambda r} {}_1F_1(-i\alpha_e, 1; i(kr + \mathbf{k}\cdot\mathbf{r})), \quad (19)$$

which is a simplified Nordsieck-type [14] integral that has in our case a simple analytical expression. Finally the three-dimensional integral in Eq. (17) is determined numerically.

III. RESULTS

We chose the domain of relatively high incident energy values (2 keV). We also fix the ejected electron energy to 50 eV, as in our first paper [12], and limit ourselves to the coplanar geometry, where the internuclear axis, the incidence, scattering, and the ejection directions are in the same plane.

We begin by giving in Fig. 2 an overall image of the variation of the sevenfold differential cross section (7DCS) for a fixed direction of the molecular axis $\theta_\rho = 135^\circ$ and $\varphi_\rho = 0^\circ$ in terms of the ejection and the scattering angles simultaneously. This presents the same characteristics of the graphs concerning the variation of the triple differential cross section of an atomic system, with the usual Bethe ridge, where the ejection direction is parallel to that of the momentum transfer, and the binary and recoil structures for small scattering angles, which are obtained when the recoil momentum of the target is optimal. Now comparing in this situation our results for a particular, small scattering angle $\theta_s = 1^\circ$ to that obtained by Messiah's model in Fig. 3 we see that the TCC model favors the binary region, in contrast with Messiah's model, which favors the back ejection region like in the atomic case. This difference in the behavior can be explained by the nature of the two models, as Messiah's model considers the molecular transition matrix element [Eq. (15) of [12]] as a combination of simple products of $e^{\pm i\mathbf{K}\cdot\boldsymbol{\rho}}$ with one-center transition matrices, in contrast with the TCC model in which the ejected electron "belongs" to the molecule as a whole. Now as \mathbf{K} is small for small scattering angles and hence $e^{\pm i\mathbf{K}\cdot\boldsymbol{\rho}} \approx 1$, the results obtained by Messi-

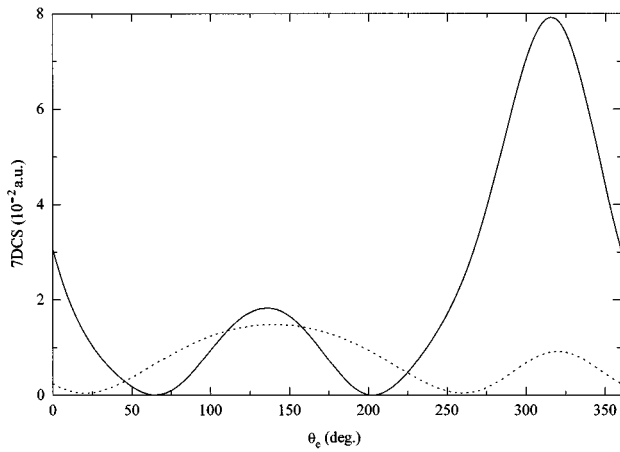


FIG. 3. The sevenfold differential cross section (7DCS) of the $(e,2e)$ ionization of H_2^+ in terms of the ejection angle, θ_e . The incident and the ejected electron energies are 2 and 50 keV, respectively, the scattering angle $\theta_s=1^\circ$ and $\theta_p=135^\circ$. The full line gives the results obtained by the two-center continuum model, and the dotted line those obtained by Messiah's model.

ah's model have in this situation an atomic character (Fig. 3).

To study in more detail the molecular aspect of our problem we show in Fig. 4 the variation of the 7DCS in terms of the orientation of the molecule θ_p , and the scattering angle θ_s , simultaneously for $\varphi_p=0^\circ$ and fixed incident energy of 2 keV. The ejection direction here is taken parallel to that of the momentum transfer, which itself varies slowly with θ_s . Three domains for the scattering angle appear. The first, for small angles between 0° and 4° , second, for intermediate values, between 5° and 15° , and finally the large scattering angle region, which goes from the intermediate region to the backscattering region until $\theta_s=180^\circ$, where the 7DCS, shown in Fig. 5 for a fixed direction of the molecule, has very small values.

For the region of small scattering angles (Fig. 4), where the impact parameter is large, the 7DCS is very sensitive to θ_p , and it takes a maximal value for $\theta_p \cong 140^\circ$. In this di-

rection the molecular axis is parallel to the momentum transfer direction. Recalling the spheroidal shape of the electron cloud of the $1s\sigma_g$ state, this result seems physically plausible as the velocity of the bound electron is oriented in this direction. Now in Messiah's model, the conclusion is the same, but with smaller sensitivity to θ_p for the same reason as above, showing that the molecular aspect of the problem for this model should be small as the momentum transfer is small.

In the intermediate values of θ_s , we are in, what we call in the atomic case, the Bethe region, where the momentum transfer is relatively large (> 1 a.u.) and where the maximum 7DCS is obtained at zero recoil momentum of the target, for the situations where the momentum transfer \mathbf{K} is equal and parallel to the momentum of the ejected electron \mathbf{k}_e , as

$$\mathbf{K} = \mathbf{k}_i - \mathbf{k}_s = \mathbf{k}_e + \mathbf{k}_{\text{recoil}}. \quad (20)$$

Now the Bethe ridge is found at $\theta_s=9^\circ$ for the given energy values. It is interesting to see that in our case, in Fig. 4, the maximum does not occur at the same position when the molecule is turned around. This means also that the zero of the recoil momentum of the center of mass of the molecule is not, like in the atomic case, the most favorable situation for the ionization in the momentum transfer direction.

It is also interesting to observe that in this region the 7DCS is not very sensitive to θ_p , with a small advantage given to the direction of the internuclear axis parallel to the scattering direction. This means that the ejection in the momentum transfer direction is most probable when the molecular axis is parallel to scattering the direction. This difference of behavior of the 7DCS between the small and medium scattering angle domain could be explained by the fact that in this region the interaction terms between the incident electron and the nuclei are small, and that the interaction with the target electron prevails. Moreover, the recoil momentum is very small in this region, which means that all the momentum is transferred to the target electron. Now the incident electron is nearer to the electron cloud, as the impact parameter is smaller here, so it will have a greater chance of

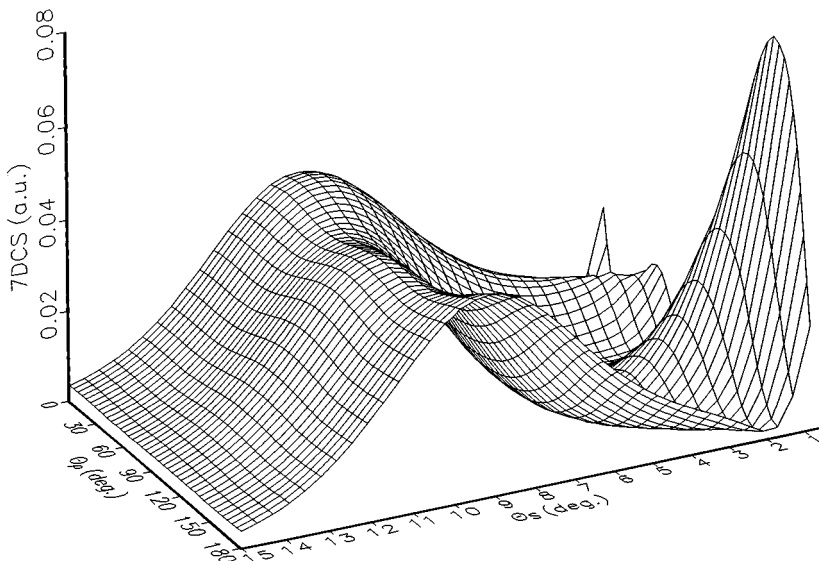


FIG. 4. The sevenfold differential cross section (7DCS) of the $(e,2e)$ ionization of H_2^+ in terms of the internuclear axis direction θ_p and scattering angle θ_s . The incident and the ejected electron energies are 2 keV and 50 eV, respectively. The ejection direction is taken parallel to the momentum transfer direction.

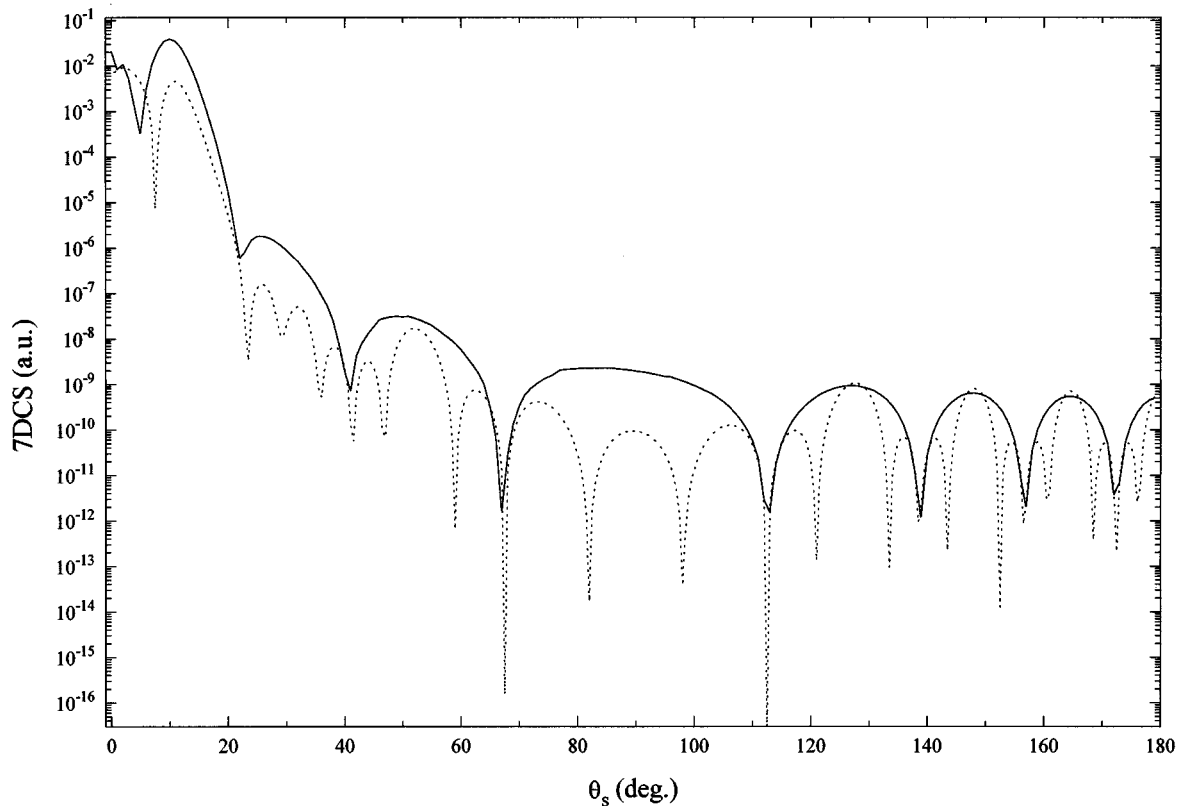


FIG. 5. The sevenfold differential cross section (7DCS) of the $(e, 2e)$ ionization of H_2^+ in terms of the scattering angle θ_s . The incident and the ejected electron energies are 2 keV and 50 eV, respectively. The ejection direction is taken parallel to the momentum transfer and $\theta_\rho = 90^\circ$. The full line gives the results obtained by the two-center continuum model, and the dotted line those obtained by Messiah's model.

interacting with the target electron when the molecule is somewhat aligned in its direction.

To study the third domain for large scattering angles ($15^\circ < \theta_s < 180^\circ$), we will consider the variation of the 7DCS in two different situations. First we will fix the orientation of the internuclear axis perpendicular to the incidence direction ($\theta_\rho = 90^\circ$). Figure 5 shows this variation compared to that obtained by Messiah's model. In spite of the fact that the values of the 7DCS are very small with respect to those of the small scattering angle region, these curves reveal interesting "diffraction" patterns, whose interfringe depends on the incident energy value and the direction of the internuclear axis. Now the "diffraction and interference pattern" obtained by Messiah's model looks like that obtained by two optical apertures. This is an expected result when we observe the transition matrix element (Eq. (15) of [12]). Now the diffraction pattern obtained by the TCC model presents the characteristic of that obtained by one optical aperture, as here the molecule is considered as a whole, and the atomic aspect of the problem is less pronounced because of the TCC description of the ejected electron, which mixes up, as shown in Eq. (14), the effect of the two centers. It should be mentioned here, that a particular structure is observed around 90° . We have observed that, when the orientation of the internuclear axis is changed, this central structure follows the new direction. This could be a very practical indication about the direction of the molecular axis of linear targets.

A second interesting situation in this domain of large scattering angles is obtained when the direction of the internu-

clear axis is taken perpendicular to the momentum transfer, the ejection electron coming out always parallel to the momentum transfer. In this situation the recoil momentum, which is parallel to momentum transfer, will be perpendicular to the molecular axis and thus the molecule will behave like an atom and its Bethe ridge will coincide with that of the atom. Figure 6 shows this variation for the two methods, where we see that the diffraction patterns disappear in the two cases and the Bethe ridge is exactly at 9° .

IV. CONCLUSION

We have developed a procedure to determine the sevenfold differential cross section of the dissociative simple ionization of diatomic systems using, for the ejected electron, a continuum description, which satisfies the correct boundary conditions. The results of our calculations for the case of fast incident electrons show that the momentum transfer plays a role similar to that in the atomic case. By varying the direction of the molecular axis and the scattering angle we have revealed the molecular aspects of this problem and observed diffraction and interference patterns of the 7DCS curves.

ACKNOWLEDGMENTS

The authors would like to thank the CIRIL (Centre Inter-universitaire de Ressources Informatiques Lorrain) and the CNUSC (Centre National Universitaire Sud de Calcul) for the allocation of computer time.

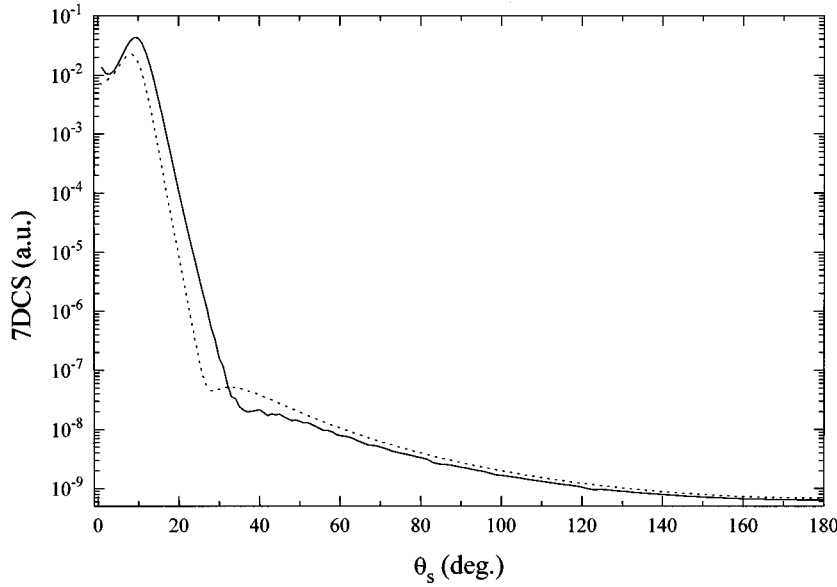


FIG. 6. The same as Fig. 5, but here the internuclear axis is always perpendicular to the ejection direction, which is parallel to the momentum transfer direction.

APPENDIX

Determination of the integral [Eq. (17)]

$$I_j(a,b) = \int \frac{d\mathbf{R}}{R_j} d\mathbf{r} e^{i\mathbf{K}\cdot\mathbf{R}} e^{-i\mathbf{k}_e\cdot\mathbf{r}} e^{-ar_1} \times {}_1F_1(-i\alpha_e, 1; i(k_e r_1 + \mathbf{k}_e \cdot \mathbf{r}_1)) e^{-br_2} \times {}_1F_1(-i\alpha_e, 1; i(k_e r_2 + \mathbf{k}_e \cdot \mathbf{r}_2)). \quad (\text{A1})$$

Let us consider the function

$$\Gamma(\mathbf{r}_1) = e^{-ar_1} {}_1F_1(-i\alpha_e, 1; i(k_e r_1 + \mathbf{k}_e \cdot \mathbf{r}_1)) = \frac{1}{(2\pi)^{3/2}} \int d\boldsymbol{\tau} \Psi(\boldsymbol{\tau}) e^{i\boldsymbol{\tau}\cdot\mathbf{r}_1} \quad (\text{A2})$$

with

$$\Psi(\boldsymbol{\tau}) = \frac{1}{(2\pi)^{3/2}} \int d\mathbf{r}_1 \Gamma(\mathbf{r}_1) e^{-i\boldsymbol{\tau}\cdot\mathbf{r}_1}. \quad (\text{A3})$$

Importing this expression in (A1), we obtained

$$I_j(a,b) = \frac{1}{(2\pi)^{3/2}} \int \frac{d\mathbf{R}}{R_j} d\mathbf{r} e^{i\mathbf{K}\cdot\mathbf{R}} e^{-i\mathbf{k}_e\cdot\mathbf{r}} \int d\boldsymbol{\tau} \Psi(\boldsymbol{\tau}) e^{i\boldsymbol{\tau}\cdot\mathbf{r}_1} \times e^{-br_2} {}_1F_1(-i\alpha_e, 1; i(k_e r_2 + \mathbf{k}_e \cdot \mathbf{r}_2)). \quad (\text{A4})$$

Considering that

$$\mathbf{R} = \mathbf{R}_2 + \frac{\boldsymbol{\rho}}{2} = \mathbf{R}_1 - \frac{\boldsymbol{\rho}}{2}, \quad \mathbf{r} = \mathbf{r}_2 + \frac{\boldsymbol{\rho}}{2} = \mathbf{r}_1 - \frac{\boldsymbol{\rho}}{2}, \quad \mathbf{R}_3 = \mathbf{R} - \mathbf{r}, \quad (\text{A5})$$

we can write

$$I_j(a,b) = (2\pi)^{-3} e^{-i(\mathbf{k}_e \cdot \boldsymbol{\rho}/2)} \int d\boldsymbol{\tau} e^{i\boldsymbol{\tau}\cdot\boldsymbol{\rho}} \times \int \frac{d\mathbf{R}}{R_j} d\mathbf{r}_2 \Psi(\boldsymbol{\tau}) e^{i\mathbf{K}\cdot\mathbf{R}} e^{-i(\mathbf{k}_e - \boldsymbol{\tau})\cdot\mathbf{r}_2} e^{-br_2} \times {}_1F_1(-i\alpha_e, 1; i(k_e r_2 + \mathbf{k}_e \cdot \mathbf{r}_2)). \quad (\text{A6})$$

Now using the integral

$$\int d\mathbf{R} \frac{e^{i\mathbf{K}\cdot\mathbf{R}}}{R_j} = \frac{4\pi}{K^2} e^{i(s_j \mathbf{K} \cdot \boldsymbol{\rho}/2)} e^{i\eta_j \mathbf{K} \cdot \mathbf{r}_2} \quad (\text{A7})$$

with

$$s_j = -1, \quad \eta_j = 0 \quad \text{for } j=1,$$

$$s_j = 1, \quad \eta_j = 0 \quad \text{for } j=2,$$

$$s_j = 1, \quad \eta_j = 1 \quad \text{for } j=3, \quad (\text{A8})$$

and defining the basic integral,

$$W(\mathbf{k}, \mathbf{q}, \lambda) = \int d\mathbf{r} e^{-i\mathbf{q}\cdot\mathbf{r}} e^{-\lambda r} {}_1F_1(-i\alpha_e, 1; i(kr + \mathbf{k} \cdot \mathbf{r})), \quad (\text{A9})$$

we can write (A6) in its simpler form of Eq. (17).

- [1] Y. D. Wang, J. H. McGuire, and R. D. Rivarola, *Phys. Rev. A* **40**, 3673 (1989).
- [2] S. E. Corchs, R. D. Rivarola, J. H. McGuire, and Y. D. Wang, *Phys. Rev. A* **47**, 201 (1993).
- [3] S. E. Corchs, R. D. Rivarola, J. H. McGuire, and Y. D. Wang, *Phys. Scr.* **50**, 469 (1994).
- [4] M. Cherid, PhD thesis, Université de Paris Sud, 1988.
- [5] M. C. Dal Cappello, C. Dal Cappello, C. Tavard, M. Cherid, A. Lahman Bennani, and A. Duguet, *J. Phys. France* **50**, 207 (1989).
- [6] C. A. Coulson, *Trans. Faraday Soc.* **33**, 1479 (1937).
- [7] J. D. Power, *Philos. Trans. R. Soc. London Ser. A* **274**, 663 (1973).
- [8] M. Aubert, N. Bessis, and G. Bessis, *Phys. Rev. A* **10**, 51 (1974).
- [9] B. H. Wells and S. Wilson, *J. Phys. B* **19**, 17 (1986).
- [10] A. Messiah, *Quantum Mechanics* (Wiley, New York, 1965), Chap. XIX Sec. 24.
- [11] J. H. McGuire, *Adv. At. Mol. Opt. Phys.* **29**, 217 (1992).
- [12] J. Hanssen, B. Joulakian, R. D. Rivarola, and R. J. Allan, *Phys. Scr.* **53**, 41 (1996).
- [13] P. Pluvinage, *Phys. Radium* **12**, 789 (1951).
- [14] A. Nordsieck, *Phys. Rev.* **93**, 785 (1954).